

# AHSG: Adversarial Attacks on High-level Semantics in Graph Neural Networks

Kai Yuan<sup>1</sup>, Xiaobing Pei<sup>1</sup>, Haoran Yang<sup>1</sup>

<sup>1</sup>Huazhong University of Science and Technology  
m202376878@hust.edu.cn, xiaobingp@hust.edu.cn, m202276630@hust.edu.cn.

## Abstract

Graph Neural Networks (GNNs) have garnered significant interest among researchers due to their impressive performance in graph learning tasks. However, like other deep neural networks, GNNs are also vulnerable to adversarial attacks. In existing adversarial attack methods for GNNs, the metric between the attacked graph and the original graph is usually the attack budget or a measure of global graph properties. However, we have found that it is possible to generate attack graphs that disrupt the primary semantics even within these constraints. To address this problem, we propose a Adversarial Attacks on High-level Semantics in Graph Neural Networks (AHSG), which is a graph structure attack model that ensures the retention of primary semantics. The latent representations of each node can extract rich semantic information by applying convolutional operations on graph data. These representations contain both task-relevant primary semantic information and task-irrelevant secondary semantic information. The latent representations of same-class nodes with the same primary semantics can fulfill the objective of modifying secondary semantics while preserving the primary semantics. Finally, the latent representations with attack effects is mapped to an attack graph using Projected Gradient Descent (PGD) algorithm. By attacking graph deep learning models with some advanced defense strategies, we validate that AHSG has superior attack effectiveness compared to other attack methods. Additionally, we employ Contextual Stochastic Block Models (CSBMs) as a proxy for the primary semantics to detect the attacked graph, confirming that AHSG almost does not disrupt the original primary semantics of the graph.

## Introduction

Graph structures are used to model many real-world relationships, such as molecular structures (Dai et al. 2019), social relationships (Bian et al. 2020), network flows (Shen et al. 2022), and transportation (Zhou et al. 2023). Learning effective representations of graphs and applying them to solve downstream tasks has become increasingly important. In recent years, GNNs (Kipf and Welling 2017; Veličković et al. 2018; Hamilton, Ying, and Leskovec 2017) have achieved significant success in graph representation learning. GNNs follow the message-passing mecha-

nism (Gilmer et al. 2017), where node embeddings are obtained by aggregating and transforming the embeddings of their neighbours. Due to their excellent performance, GNNs have been applied to various analytical tasks, including node classification (Jin et al. 2021a; Wu, Pan, and Zhu 2021), link prediction (Xiong et al. 2022; Ma et al. 2020), and graph classification (Gao et al. 2021; Errica et al. 2022).

GNNs have achieved significant breakthroughs in many graph-related tasks. However, recent studies have shown that similar to traditional deep neural networks, GNNs suffer from poor robustness when facing specially designed adversarial attacks. Attackers can generate graph adversarial perturbations to deceive GNNs by manipulating graph structures and node features (Dai et al. 2018; Xu et al. 2019; Zügner and Günnemann 2019; Zügner, Akbarnejad, and Günnemann 2018; Liu et al. 2022; Zhang et al. 2022), or generating new nodes and adding them to the original graph (Fang et al. 2024; Chen et al. 2022). By understanding the ways in which models are vulnerable to attacks, researchers can design more robust models (Zhu et al. 2019; Wu et al. 2019; Jin et al. 2020, 2021b; Entezari et al. 2020) that perform better when confronted with adversarial samples.

A core principle of attacking neural networks is that the attacker should preserve the primary semantics of the original data after adding perturbations. In other words, human observers should perceive the samples before and after perturbation as semantically equivalent. For example, an image should still be recognized by humans as the same object even after perturbation. This semantic invariance ensures the practical significance of the attack. To achieve semantic invariance in adversarial examples, adversarial attacks usually require the attacker to make only minimal perturbations. Therefore, most existing research on graph adversarial attacks (Dai et al. 2018; Xu et al. 2019; Zügner and Günnemann 2019; Zügner, Akbarnejad, and Günnemann 2018; Liu et al. 2022) restricts the attacker to modify only a limited number of edges or nodes. This limitation is known as the attack budget. These studies assume that within a limited attack budget, the semantics of the adversarial example do not change. However, it is questionable whether attack models of the kind are able to preserve the primary semantics. For example, the proportion of low-degree nodes is large in real-world graphs, and small attack budget still allows the original neighbours of low-degree nodes to be

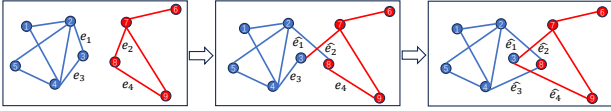


Figure 1: The primary semantics of graph are disrupted under the constraints of degree distribution.

completely deleted. Once the edges of low-degree nodes are destroyed, the semantics of these nodes are likely to be destroyed. It is not enough to limit the change of semantics only by using the attack budget. To further constrain semantic changes, a few studies have introduced metrics beyond attack budget limitations. (Zügner, Akbarnejad, and Günnemann 2018; Chen et al. 2022) suggest using different global graph properties as proxies for semantics, such as degree distribution (Zügner, Akbarnejad, and Günnemann 2018) and homophily (Chen et al. 2022). However, we find that even under such constraints, the primary semantics can still be disrupted. Figure 1 illustrates this phenomenon with a binary classification task. Assume we have an undirected graph. Select any two edges  $e_1 = (i, j)$  and  $e_2 = (u, v)$  from the edge set of the graph. Now, we replace the two edges with  $\hat{e}_1 = (i, v)$  and  $\hat{e}_2 = (u, j)$ . Since  $\deg(i)$ ,  $\deg(j)$ ,  $\deg(u)$ , and  $\deg(v)$  remain unchanged, this process preserves the degree distribution of the graph. We can continue to modify the edges according to Figure 1 until the attack budget is exhausted. We successfully modifies the semantics of nodes 3 and 8 in Figure 1 while maintaining the overall graph distribution, demonstrating the infeasibility of method (Zügner, Akbarnejad, and Günnemann 2018). Therefore, neither the attack budget nor the additional constraints on graph properties can effectively preserve the primary semantics of the graph. Current research lacks the fundamental constraint of maintaining primary semantics. To address this issue, we propose a high-level semantic adversarial attack targeting graph neural networks. This method aims to generate attack graphs that preserve primary semantics within limited attack budget.

The semantics of the graph is contained in the latent representations of graph neural network, so we control the change of the latent representations to control the semantic change of the attacked graph. Existing attack methods (Dai et al. 2018; Xu et al. 2019; Zügner and Günnemann 2019; Zügner, Akbarnejad, and Günnemann 2018; Liu et al. 2022; Zhang et al. 2022) often treat graph neural networks as black boxes, focusing only on the input and output, while ignoring the rich semantic information contained in the hidden layer (its own node features as well as the structural information of the surrounding neighborhood). While many of them represent the primary semantics of an object in a fixed task, some of them are secondary. For example, in social networks, the height of person nodes is secondary to the task of predicting friend relationships, while the interests of person nodes are primary. These secondary semantics may play an inappropriately important role in the model predictions. In an ideal situation, the construction of adversarial examples should lead the model to misjudge through exploring and exploiting

the secondary semantics while keeping the primary semantics unchanged.

We endeavor to seek the attacked graph which preserves the primary semantics from the latent representations that contain semantics. Subsequently, how can we acquire the latent representations where primary semantics remain unchanged while secondary semantics change? Nodes of the same class have similar primary semantics in a fixed task, so a linear combination of representations of them can still retain their primary semantics. We use the latent representations after linear combination as input to the lower network, then use gradient ascent to find latent representations with attack effects. To generate adversarial samples, a first-order optimization algorithm is employed to map the perturbed latent representations with attack effects to the attacked graph. Finally, extensive experiments validate the attack performance of AHSG on different datasets and against different defense methods.

Our main contributions are as follows:

- To overcome the challenge of preserving primary semantics in attacked graph, we propose a new strategy based on a novel perspective of latent semantic representations in graph neural network, which cleverly utilizes the same-class latent representations with similar primary semantics as the perturbation range.
- In the setting of evasion attacks, we introduce AHSG. By extracting continuous latent representations from discrete graph data through convolutional operations, we perform a linear combination of same-class node representations as perturbations. Then, we use a first-order optimization algorithm to reconstruct adversarial samples from the perturbed representations.
- Through comprehensive experiments on multiple acknowledged benchmark datasets, we compare AHSG with current advanced attack models and use various defense models for evaluation. The results demonstrate that AHSG achieves excellent attack performance under different attack budgets. Furthermore, semantic detection experiments confirm that AHSG preserves the primary semantics of graph data in fixed tasks.

## Preliminary

Given an undirected attributed graph  $G = (A, X)$  with  $n$  nodes, where  $A \in \{0, 1\}^{n \times n}$  represents the adjacency matrix, and  $X \in \mathbb{R}^{n \times d}$  represents the node feature matrix. Here,  $d$  represents the feature dimension, and  $n$  represents the total number of nodes. We focus on an undirected attributed graph in this work. Formally, we denote the set of nodes as  $V = \{v_i\}$  and the set of edges as  $E \subseteq V \times V$ . Each node  $v_i$  is associated with a corresponding node label  $y_i \in Y = \{0, 1, \dots, c-1\}$ , where  $c$  is the total number of labels.

## GCN

Graph Convolutional Network (GCN) (Kipf and Welling 2017) is one of the classic models based on graph learning and has been widely applied to various tasks. The principle of GCN involves a message passing mechanism, where each

node updates its representation by aggregating information from itself and its neighboring nodes using pre-defined deterministic rules (e.g., Laplacian matrix, adjacency matrix, and attention). The process of message passing can be represented as follows:

$$H^{(l+1)} = \sigma(\tilde{D}^{-\frac{1}{2}} \tilde{A} \tilde{D}^{-\frac{1}{2}} H^{(l)} W_{(l)}). \quad (1)$$

Here, the node representation  $H^{(l)}$  is updated to  $H^{(l+1)}$  after message passing. In Equation (1),  $\tilde{A} = A + I_N$  and  $\tilde{D}_{ii} = \sum_j \tilde{A}_{ij}$ , where  $\tilde{D}_{ii}$  is equal to the degree of node  $v_i$  plus 1.  $\sigma(\cdot)$  is a non-linear activation function, such as ReLU. The initial node representation  $H^{(0)}$  is set to the node features  $X$ .  $W_{(l)}$  ( $l = 1, 2, \dots, L$ ) are the weight matrices. Typically, a fully connected layer with a softmax function is used for classification after  $L$  graph convolutions. Generally, a two-layer GCN is considered for node classification tasks. Thus, the model can be described as:

$$Z = f(G(X, A)) = \text{softmax}(\hat{A} \sigma(\hat{A} X W_{(1)}) W_{(2)}), \quad (2)$$

where  $\hat{A} = \tilde{D}^{-\frac{1}{2}} \tilde{A} \tilde{D}^{-\frac{1}{2}}$  is the symmetrically normalized adjacency matrix.

### Graph Adversarial Attack

Graph adversarial attack aims to make graph neural networks produce incorrect predictions. It can be described by the following formulation:

$$\begin{aligned} \max_{\hat{G} \in \Phi(G)} L(f_{\theta^*}(\hat{G}(\hat{A}, \hat{X})), Y) \\ \text{s.t. } \theta^* = \arg \min_{\theta} L(f_{\theta}(G'(A', X')), Y). \end{aligned} \quad (3)$$

Here,  $f$  can be any learning task function on the graph, such as node-level embedding, node-level classification, link prediction, graph-level embedding, or graph-level classification. In this paper, we primarily focus on node-level classification.  $\Phi(G)$  represents the perturbation space on the original graph  $G$ . The distance between the adversarial graph and the original graph is typically measured using the attack budget or other properties. The graph  $\hat{G}(\hat{A}, \hat{X})$  represents the adversarial sample.

When  $G'$  is equal to  $\hat{G}$ , Equation (3) represents poisoning attack. Poisoning attack occurs during model training. It attempts to influence the model's performance by injecting adversarial samples into the training dataset. On the other hand, when  $G'$  is the unmodified original  $G$ , Equation (3) represents evasion attack. Evasion attack occurs after the model is trained, meaning that the model's parameters are fixed when the attacker executes the attack. The attacker aims to generate adversarial samples specifically for the trained model. AHSg attacks the target model after its training, which categorizes it as an evasion attack.

### Methodology

In this part, we first derive the formulation of the proposed model and then present its optimization algorithm.

#### Model establishment

As shown in Figure 2, AHSg can be divided into three stages:

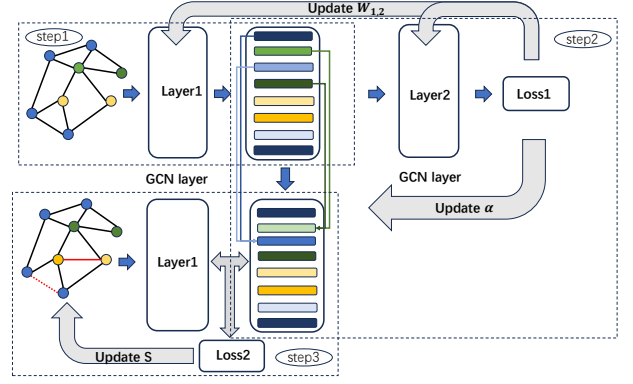


Figure 2: The framework of AHSg. We use the same color scheme to represent latent representations of same-class nodes. The color indicates primary semantics, while color depth represents secondary semantics.

**1) Extract semantics from graph:** The hidden layers of an unperturbed surrogate GCN encapsulate both the information of the node itself and that of its surrounding neighborhood after training. Therefore, we consider the output from the first convolutional layer and activation function as the semantics of each node. This process can be formally described as follows:

$$\begin{aligned} H_1 = \sigma(n(A) X W_{(1)}^*) \\ \text{s.t. } W_{(1,2)}^* = \arg \min_{W_{(1,2)}} L(f_{W_{(1,2)}}(G(A, X)), Y), \end{aligned} \quad (4)$$

where  $f_{W_{1,2}}(G(A, X))$  is a shorthand for the expression in Equation (2),  $L(\cdot, \cdot)$  is the loss function, commonly the cross-entropy loss.  $n(A) = \tilde{D}^{-\frac{1}{2}}(A + I)\tilde{D}^{-\frac{1}{2}}$ .

**2) Construct adversarial latent representation that preserve the primary semantics:** (Wang et al. 2021) addresses the challenge of imbalanced datasets by extracting the feature shifts of frequent-class entities and applying them to rare-class entities. In this approach, the latent representation is assumed to be  $h = P + T$ , where  $P$  denotes the data distribution center (i.e., the similar primary semantics of same-class entities under the fixed task), and  $T$  represents the feature shift (i.e., the secondary semantics of the entities in the task). Inspired by this, we make the following assumption about the composition of the latent representation in our work:

$$h_j^i = dP(i) + eT(j), \quad (5)$$

where  $h_j^i$  denotes the latent representation vector of the  $j$ -th node in class  $i$ . It is composed of two parts: the primary semantics  $eP(i)$ , which is crucial for the classification task, and the secondary semantics  $fT(j)$ , which is less decisive. All nodes of the same class share the same primary semantic base  $P(i)$ , but may have different secondary semantic bases  $T(j)$ . Since each class contains some nodes, there exists a set where the primary semantics are preserved while the secondary semantics change. When perturbing the latent representation  $h_j^i$  of each node, we assign a weight  $\alpha_k$  to each

representation of the same class. Summing these weighted representations yields the perturbed representation  $\hat{h}_j^i$ .

$$\hat{h}_j^i = \frac{\sum_{k=1}^j \alpha_k h_k^i}{\sum_{k=1}^j \alpha_k}. \quad (6)$$

From Equation (5), the representation  $\hat{h}_j^i$  can be derived as follows:

$$\begin{aligned} \hat{h}_j^i &= \frac{\sum_{k=1}^j \alpha_k h_k^i}{\sum_{k=1}^j \alpha_k} \\ &= \frac{\sum_{k=1}^j \alpha_k (d_k P(i) + e_k T(k))}{\sum_{k=1}^j \alpha_k} \\ &= \frac{\sum_{k=1}^j \alpha_k d_k P(i) + \sum_{k=1}^j \alpha_k e_k T(k)}{\sum_{k=1}^j \alpha_k} \\ &= \left( \frac{\sum_{k=1}^j \alpha_k d_k}{\sum_{k=1}^j \alpha_k} \right) * P(i) + \frac{\sum_{k=1}^j \alpha_k e_k T(k)}{\sum_{k=1}^j \alpha_k}. \end{aligned} \quad (7)$$

As derived above,  $\hat{h}_j^i$  still maintains the form  $dP + eT$ , where the secondary component is composed of various secondary semantics, and the primary component remains but with a modified coefficient for the primary semantics base. To ensure that the perturbed latent representation  $\widehat{H}_1$  has adversarial effect on the GCN,  $\widehat{H}_1$  is fed into the downstream network layers of the GCN. The optimal  $\alpha$  is then determined based on the loss function  $\text{loss}_1$ .  $[h]$  refers to arranging  $h$  in the same order as before.

$$\text{loss}_1 = -L(Y, \text{softmax}(n(A)\widehat{H}_1(\alpha)W_{(2)}^*)) - \beta \text{sim}(H_1, \widehat{H}_1(\alpha)). \quad (8)$$

$$\widehat{H}_1(\alpha) = [\hat{h}_j^i] = \left[ \frac{\sum_{k=1}^j \alpha_k h_k^i}{\sum_{k=1}^j \alpha_k} \right]. \quad (9)$$

To use a smaller attack budget when reconstructing adversarial samples with perturbed representations, we introduce a penalty term  $\text{sim}(H_1, \widehat{H}_1(\alpha))$ . This term controls the similarity between the perturbed hidden layer and the original hidden layer, thereby limiting the perturbations to a certain range. Notably, it also prevents the coefficient of the primary semantics base from becoming too small.  $\beta > 0$  is a hyperparameter that controls the strength of the penalty.

### 3)Map adversarial latent representation to adversarial sample:

To construct an adversarial sample, we need to map the perturbed latent representation to the graph. Let  $\hat{A}$  denote the attacked graph. We introduce a boolean symmetric matrix  $S \in \{0, 1\}^{N \times N}$  to encode whether an edge in  $G$  is modified. Specifically, an edge  $(i, j)$  is modified (added or removed) if  $S_{ij} = S_{ji} = 1$ . Otherwise, if  $S_{ij} = S_{ji} = 0$ , the edge  $(i, j)$  remains undisturbed. Given the adjacency matrix  $A$ , its complement matrix  $\bar{A}$  is defined as  $\bar{A} = 11^T - I - A$ , where  $I$  is the identity matrix, and  $1$  is a column vector of all ones. The term  $(11^T - I)$  corresponds to a fully connected graph. Using the edge perturbation matrix  $S$  and the

complement matrix  $\bar{A}$ , Equation (10) provides the perturbed topology  $\hat{A}$  of the graph  $A$ .

$$\hat{A} = A + C \odot S, \quad C = \bar{A} - A. \quad (10)$$

In Equation (10),  $\odot$  denotes the element-wise product. In the above expression, the positive entries of  $C$  indicate edges that can be added to the graph  $A$ , while the negative entries of  $C$  indicate edges that can be removed from  $A$ . Due to the difficulty in solving the problem under the binary constraint  $\{0, 1\}$ , this constraint is relaxed to the continuous interval  $[0, 1]$ . Based on Equation (4), the latent representation is computed by using the modified graph structure  $\hat{A}$ . It is then made similar to  $\widehat{H}_1$ .

$$\text{loss}_2 = -\text{sim}(\sigma(n(\hat{A})XW_{(1)}^*), \widehat{H}_1) \text{ s.t. } s \in S. \quad (11)$$

where  $S = \{s \mid 1^T s \leq \epsilon, s \in [0, 1]^{N^2}\}$ . The function  $\text{sim}(\cdot, \cdot)$  computes the distance between matrices, commonly using KL divergence. After determining  $s$  based on  $\text{loss}_2$ , the values in  $s$  are used to sample from  $\hat{A}$ , resulting in the perturbed graph  $\hat{A}$ .

### Model Optimization

We solve AHSG step by step. In the first step, we solve for  $W$  by using a conventional gradient descent algorithm. In the second step, when solving the  $\alpha$  problem, the number of elements in  $\alpha$  corresponding to each node is variable because the number of same-class nodes for each node is not fixed. It is challenging to solve for unknowns of variable length in a unified manner. However, the maximum length of  $\alpha$  is fixed, which is the total number of nodes. We set each  $\alpha$  to the maximum length, and after each gradient descent iteration, we perform clipping according to the following formula:

$$\tau(\alpha_{i,j}) = \begin{cases} 1, & \text{if } (i = j \text{ and } y_i \text{ is unknown}) \\ \alpha_{i,j}, & \text{if } (y_i = y_j \text{ and } y_i \text{ and } y_j \text{ are known}) \\ 0, & \text{else} \end{cases}. \quad (12)$$

For the  $s$  subproblem, we scale the hard constraints  $\{0, 1\}$  to  $[0, 1]$ . However, under the constraint  $1^T s \leq \epsilon$ , we still need to project the gradient-descent result of  $s$  by Equation (13). For solving  $\mu$ , we use the bisection method.

$$\Pi_S(a) = \begin{cases} P_{[0,1]}[a], & \text{if } \sum P_{[0,1]}[a] \leq \epsilon \\ P_{[0,1]}[a - \mu], & \text{if } \mu > 0, \sum P_{[0,1]}[a - \mu] = \epsilon \end{cases}. \quad (13)$$

where  $P_{[0,1]}(x)$  is defined as:

$$P_{[0,1]}(x) = \begin{cases} x, & \text{if } x \in [0, 1] \\ 1, & \text{if } x > 1 \\ 0, & \text{if } x < 0 \end{cases}. \quad (14)$$

Sampling  $A$  using  $s$  produces the attacked graph  $\hat{A}$ . The pseudo-code of AHSG is shown in Algorithm 1.

## Experiment

In this section, we validate the effectiveness of AHSG through comprehensive experiments. First, we will introduce the experimental setup, including dataset statistics, baselines, GNNs, and parameter settings. Next, we present the experimental results and analyze them to verify the performance and characteristics of AHSG.

### Dataset

We evaluated AHSG on three well-known datasets: Cora, Citeseer, and Cora-ML. All datasets contain unweighted edges, allowing the generation of an adjacency matrix  $A$ , and include sparse bag-of-words feature vectors that can be used as input for GCN. Among them, Cora and Citeseer are symmetric matrices (i.e., undirected graphs), while Cora-ML is an asymmetric matrix (i.e., directed graph). For this experiment, we converted the Cora-ML dataset into an undirected graph. The Cora and Citeseer datasets have binary features, while the Cora-ML dataset contains continuous features. Following the setup from previous work (Kipf and Welling 2017), the feature vectors of all nodes are fed into the GCN, with only 140 and 120 training nodes for Cora and Citeseer, respectively, and 200 training nodes for the Cora-ML dataset. The number of test nodes is 1,000 for all three datasets. The statistical results are shown in Table 1.

Datasets	Nodes	Links	Features	Classes	Binary
Cora	2708	5278	1433	7	Y
Citeseer	3327	4552	3703	6	Y
Cora-ML	2995	8158	2879	7	N

Table 1: Statistics of datasets. The last column indicates whether the dataset has binary features.

### Baselines and GNNs

The baselines include Random and DICE (Waniek et al. 2018), which are based on random sampling, as well as Meta-Self (Zügner and Günnemann 2019), PGD (Xu et al. 2019), and GradArgmax (Dai et al. 2018). Meta-Self employs meta-learning to attack node classification models. PGD proposes a topology attack framework based on edge perturbation, which overcomes the challenge of attacking discrete graph structures from a first-order optimization perspective. GradArgmax modifies one edge in the current graph at a time using a gradient-based greedy algorithm, and iterates until the attack budget is exhausted.

We use AHSG and the aforementioned baselines to attack GCN and five defense or robust GNN models. Jaccard (Wu et al. 2019) calculates the Jaccard similarity of connected node pairs and retains only those links with high similarity. Svd (Entezari et al. 2020) utilizes low-order approximations of the graph to enhance the performance of GCN against adversarial attacks. ProGNN (Jin et al. 2020) jointly learns the graph structure and a robust GNN model from the perturbed graph. The SimPGCN (Jin et al. 2021b) framework enhances GCN robustness by effectively preserving node similarity.

---

### Algorithm 1: AHSG

---

**Input:** Original graph  $G = (A, X)$

**Parameter:**  $L, \lambda, \beta, T, \eta_t, K, h$

**Output:**  $\hat{A}$

- 1: Train GCN to obtain  $W_{(1,2)}^*$ .
  - 2: Calculate  $H_1$  via Equation(4).
  - 3: **for**  $l \leftarrow 1$  to  $\underline{L}$  **do**
  - 4:   Calculate  $\widehat{H}_1$  via Equation(9).
  - 5:   Gradient descent:  
 $\alpha(l) = \alpha(l-1) - \lambda \nabla \text{loss}_1(\alpha(l-1))$ .
  - 6:   Calculate  $\alpha$  via Equation(12).
  - 7: **end for**
  - 8: **for**  $t \leftarrow 1$  to  $T$  **do**
  - 9:   Gradient descent:  
 $a(t) = s(t-1) - \eta_t \nabla \text{loss}_2(s(t-1))$
  - 10:   Call projection operation in Equation(13).
  - 11: **end for**
  - 12: **for**  $k \leftarrow 1$  to  $K$  **do**
  - 13:   Generate  $p$  of the same size as  $s$  that follows a uniform distribution.
  - 14:   Draw binary vector  $d^{(k)}$  following  

$$d_i^{(k)} = \begin{cases} 1, & \text{if } s_i > p_i \\ 0, & \text{if } s_i \leq p_i \end{cases}$$
  - 15: **end for**
  - 16: Choose a vector  $s^*$  from  $d^{(k)}$  which yields the smallest  $\text{loss}_2$  under  $1^T s \leq \epsilon$ .
  - 17: Calculate  $\hat{A}$  via Equation(10).
- 

RGCN (Zhu et al. 2019) proposes that latent representations based on Gaussian distributions can effectively absorb the impact of adversarial attacks.

### Experimental Setup

We conduct comparative experiments with advanced graph attack and defense methods. For Svd and Jaccard, we adjust the order of high-order approximations and the threshold for removing low-similarity links to achieve optimal defense performance. Other attack methods use default parameters. In our method, the default settings are as follows: the number of iterations  $L$  for perturbation is set to 300, with a learning rate  $\lambda$  of 0.3. The regularization coefficient  $\beta$  is 0.2. For reconstruction, the number of iterations  $T$  is 300, and the dynamic learning rate  $\eta_t$  is  $\frac{q}{\sqrt{t+1}}$ , where  $t$  denotes the iteration count and  $q$  is set to 20. The number of selections  $K$  for the probability matrix is 20. When using a two-layer GCN as the victim model, the dimension  $h$  of the first layer is 128, and the second layer’s dimension corresponds to the number of classes. In CSBMs, the number of generated nodes  $n$  is 1000. Node feature mean  $\mu$  is calculated as  $\frac{M\sigma}{2\sqrt{d}}$ , with variance  $\sigma = 1$ ,  $d = \frac{n}{(\ln(n))^2} = 21$ , and  $M = 0.5$ . Smaller value of  $M$  causes the reference classifier to rely more on structural information. Since AHSG focuses on structural attacks, it is essential for the reference classifier to analyze the semantics within the structure. The edge probability  $p$  between same-class nodes is 0.6326%, while the edge probability  $q$  between different-class nodes

is 0.1481%.

### Attack performance on GNNs

Except for ProGNN, other GNNs use the evasion attack setting. ProGNN performs both graph structure purification and parameter learning simultaneously, so the attack occurs before training. The attack results on different GNNs by modifying 10% of the edges are shown in Table 2. We observe that all baseline methods lead to a performance drop in the victim models. AHSG outperforms all other attackers on all datasets. Furthermore, AHSG achieves the best attack performance on GCN among different GNN models, as GCN is the corresponding surrogate model, indicating a white-box attack scenario. Additionally, even against the five defensive GNNs, AHSG still demonstrates strong attack performance, highlighting its robust generalization capability derived from the surrogate GCN model.

### Attack Performance w.r.t attack budget

Table 3 presents the accuracy on the test sets on three datasets as the proportion of perturbed edges increases from 5% to 20%. For example, in the case of the Cora dataset, as anticipated, the test accuracy consistently decreases with a higher number of perturbed edges, although the rate of decline slows down. Moreover, the proposed AHSG achieves the best attack performance across all perturbation ratios. Similar conclusions are drawn for the Citeseer and Cora-ML datasets.

### Semantic Detection

In the fields of computer vision (CV) and natural language processing (NLP), humans can effectively perform semantic checks. However, in the domain of graph, it is challenging for humans to inspect the semantics of large-scale graphs. To address this, (Gosch et al. 2023) attempts to define semantic boundaries by introducing a reference classifier  $g$  to represent changes in semantic content. The reference classifier  $g$  can be derived from knowledge about the data generation process. According to the data generation process of CSBMs, (Gosch et al. 2023) uses a Bayes classifier as  $g$ .

Data generation process: synthetic graphs with analytically tractable distributions are generated using the Contextual Stochastic Block Models (CSBMs). It defines the edge probability  $p$  between same-class nodes and  $q$  between different-class nodes. Node features are extracted using a Gaussian model. Sampling from CSBMs can be described as an iterative process for node  $i \in n$ :

1. Sample the label  $y_i \sim \text{Ber}(1/2)$  (Bernoulli distribution).
2. Sample the feature vector  $x_i \mid y_i \sim \mathcal{N}((2y_i - 1)\mu, \sigma I)$ , where  $\mu \in \mathbb{R}^d$  and  $\sigma \in \mathbb{R}$ .
3. For all  $j \in n$ , if  $y_i = y_j$ , then sample  $A_{j,i} \sim \text{Ber}(p)$ ; otherwise, sample  $A_{j,i} \sim \text{Ber}(q)$  and set  $A_{i,j} = A_{j,i}$ .

We denote this as  $(X, A, y) \sim \text{CSBM}(n, p, q, \mu, \sigma^2)$ .

$$\begin{aligned} g(X', A')_v &= g(X, A)_v = y_v, \\ (X, A, y) &\sim \text{CSBM}(n, p, q, \mu, \sigma^2). \end{aligned} \quad (15)$$

$$G(X', A') = \text{attack}(G(X, A)). \quad (16)$$

$$g(X, A)_v = \arg \max_y (\text{Bayes}(X, A, v, y)). \quad (17)$$

$$\begin{aligned} \text{Bayes}(X, A, v, y) &= \log(p(X_v \mid y_v) + \\ \log\left(\prod_{i=0}^n p^{A[i,v](1-|y_i-y_v|)} (1-p)^{(1-A[i,v])(1-|y_i-y_v|)} \right. & (18) \\ \left. q^{A[i,v](|y_i-y_v|)} (1-q)^{(1-A[i,v])(|y_i-y_v|)}\right). \end{aligned}$$

We reclassify the nodes in the attacked graph  $G(X', A')$ , which is generated by Equation (16). If the results satisfy (15), we consider that the attack method does not significantly disrupt the semantics of node  $v$  in the graph. The number of nodes with consistent classification results before and after the attack can be regarded as the degree of graph semantics preservation. We denote this by Bayes\_maintain, as shown in Equation (17), where  $\mathbb{I}$  is an indicator function. As shown in Table 4, the Bayes reference classifier achieves 92.4% accuracy on clean graphs, validating its effectiveness as a semantic proxy. Comparison with other attack methods reveals that AHSG alters the Bayesian classification results the least, thereby maintaining the majority of the primary semantics in the classification task while achieving the best attack performance.

$$\text{Bayes\_maintain} = \frac{\sum_{i=0}^n \mathbb{I}_{g(X', A')_v = g(X, A)_v = y_v}}{n}. \quad (19)$$

### Related Work

In graph modification attack, (Zügner, Akbarnejad, and Günnemann 2018) introduced the first adversarial attack method on graph, called Nettack. (Zügner and Günnemann 2019) treated the input graph as a hyperparameter to be learned and modified one edge per iteration. (Xu et al. 2019) overcame the challenge of attacking discrete graph structure data. (Dai et al. 2018) employed reinforcement learning, gradient-based greedy algorithms, and genetic algorithms to attack GNNs in various scenarios. (Liu et al. 2022) generated unweighted gradients on the graph structure unaffected by node confidence, fully utilizing the attack budget. However, the issue of altering graph semantics during an attack has not been well addressed in previous work. Although the attack budget is minimal relative to the entire graph, it can still lead to significant changes in the semantics of the attacked graph. Some works maintained certain properties of the graph to achieve imperceptibility, such as Nettack (Zügner, Akbarnejad, and Günnemann 2018) and HAO (Chen et al. 2022). But these constraints are necessary but not sufficient conditions for preserving semantics.

### Conclusion

In this work, we study graph structure attack on GNNs under the evasion attack setting. Unlike other studies that regard attack budgets or graph properties as semantic proxies,

Dataset	Method	Clean	Random	DICE	Meta-Self	GradArgmax	PGD	AHSG
Cora	GCN	0.8230	0.8090	0.7970	0.8090	0.7160	0.7080	<b>0.6460</b>
	Jaccard	0.7860	0.7840	0.7630	0.7360	0.7120	0.7590	<b>0.6760</b>
	Svd	0.7290	0.7110	0.7070	0.6650	0.6730	0.6860	<b>0.6480</b>
	ProGNN	0.8090	0.7940	0.7740	0.6590	0.7370	0.7030	<b>0.6540</b>
	SimPGCN	0.7900	0.7820	0.7770	0.7840	0.7030	0.7280	<b>0.6820</b>
	RGCN	0.8010	0.7480	0.7450	0.7530	0.6900	0.6780	<b>0.6510</b>
Citeseer	GCN	0.6660	0.6550	0.6470	0.6500	0.5780	0.5930	<b>0.5280</b>
	Jaccard	0.6650	0.6320	0.6490	0.6450	0.6170	0.6230	<b>0.5760</b>
	Svd	0.6010	0.5930	0.5740	0.5730	0.5880	0.5650	<b>0.5580</b>
	ProGNN	0.6830	0.6250	0.6250	0.5310	0.5660	0.6030	<b>0.5300</b>
	SimPGCN	0.6560	0.6460	0.6500	0.6480	0.5850	0.6150	<b>0.5810</b>
	RGCN	0.6100	0.5790	0.5800	0.5690	0.5760	0.5730	<b>0.5340</b>
Cora-ML	GCN	0.8590	0.8510	0.8490	0.8270	0.7430	0.7910	<b>0.7330</b>
	Jaccard	0.8600	0.8390	0.8360	0.8070	0.7700	0.8280	<b>0.7620</b>
	Svd	0.8200	0.7990	0.8260	0.7940	0.7590	0.8160	<b>0.7570</b>
	ProGNN	0.8400	0.8050	0.8050	0.7910	0.7490	0.8230	<b>0.7350</b>
	SimPGCN	0.8460	0.8360	0.8390	0.8170	0.7430	0.8180	<b>0.7400</b>
	RGCN	0.8590	0.8420	0.8420	0.8310	0.7540	0.8280	<b>0.7550</b>

Table 2: Accuracy of GNNs with 10% edge modifications. The best result in each row is highlighted in bold.

Dataset	Attack Ratio	Random	DICE	Meta-Self	GradArgmax	PGD	AHSG
Cora	5%	0.814	0.805	0.814	0.765	0.756	<b>0.698</b>
	10%	0.809	0.797	0.809	0.716	0.708	<b>0.646</b>
	15%	0.795	0.777	0.805	0.685	0.681	<b>0.615</b>
	20%	0.787	0.771	0.798	0.652	0.645	<b>0.585</b>
Citeseer	5%	0.657	0.659	0.651	0.608	0.610	<b>0.565</b>
	10%	0.655	0.647	0.650	0.578	0.593	<b>0.528</b>
	15%	0.653	0.642	0.631	0.539	0.564	<b>0.495</b>
	20%	0.641	0.634	0.628	0.507	0.529	<b>0.487</b>
Cora-ML	5%	0.853	0.850	0.841	0.791	0.843	<b>0.776</b>
	10%	0.851	0.849	0.827	0.743	0.791	<b>0.733</b>
	15%	0.846	0.843	0.821	0.721	0.751	<b>0.700</b>
	20%	0.837	0.824	0.809	0.695	0.708	<b>0.685</b>

Table 3: Accuracy of GCN under different attack budgets. The best result in each row is highlighted in bold.

Method	GCN	Beyes_maintain
Clean	0.724	0.924
AHSG	0.586	0.903
Meta-Self	0.653	0.810
GradArgmax	0.632	0.802
PGD	0.607	0.832

Table 4: Accuracy of GCN and the degree of primary semantic preservation under different attack methods.

we propose AHSG, which preserves the primary semantics of the GNN’s hidden layers to maintain the overall semantics of the graph, thereby eliminating the potential for significant semantic disruption under insufficient constraints. Specifically, by leveraging the similarity of primary semantics among same-class nodes, we construct specific representations that lead to fail of GNNs while preserving primary semantics within the set of same-class nodes. For the generation of adversarial examples, we employ the PGD al-

gorithm to reconstruct the graph structure from the perturbed latent representations. Additionally, a regularization term is incorporated during the latent representations perturbation to further constrain semantic invariance by maintaining similarity to the original representations. Extensive experimental results on different datasets demonstrate the superior attack performance of the proposed AHSG on various types of GNNs, including GCN and multiple defense models. Notably, semantic detection of the attacked graph indicates that AHSG largely preserves the primary semantics relevant to the current task.

## Appendix

### Ablation Study

To further validate the effectiveness of AHSG, we conduct an ablation study to analyze the impact of its various components. Since AHSG consists of a perturbation module, a reconstruction module, and a regularization module, we performed ablation study by removing one of these modules to

assess their influence on AHSG’s performance. The regularization module is discussed in the hyperparameter analysis. The specific combinations for the ablation study are as follows: AHSG-rec refers to the version where we retain the perturbation module of AHSG but choose random connections during the reconstruction process. AHSG-hid refers to the version where we retain the reconstruction module of AHSG but apply random perturbations during the perturbation process. As shown in Table 5, the best attack performance is achieved only when both perturbation and reconstruction steps are present simultaneously. This result is reasonable. Without the guidance of the latent representation, the reconstruction step cannot capture the correct perturbation information. Conversely, without the reconstruction step, the perturbed latent representation cannot be transformed into an effective attack graph.

Modules	Cora	Citeseer	Cora-ML
Clean	0.823	0.666	0.8590
AHSG-rec	0.8090	0.6550	0.8520
AHSG-hid	0.804	0.650	0.8420
AHSG	0.698	0.565	0.7760

Table 5: Accuracy of GCN with 10% edge modifications on different modules and datasets.

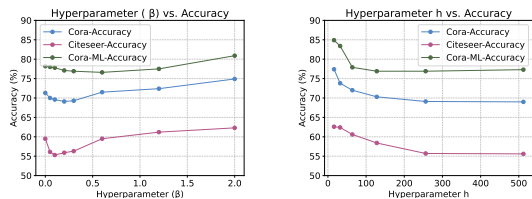


Figure 3: Hyperparameter analysis on the regularization term coefficient  $\beta$  and the hidden layer dimension  $h$ .

### Parameter Analysis

Finally, we performed a hyperparameter analysis on the regularization term coefficient  $\beta$  and the hidden layer dimension  $h$ . AHSG achieves optimal performance when  $\beta$  is around 0.1, as this value effectively balances the contributions of the attack loss and the regularization term. Large  $\beta$  restricts the range of perturbation in the hidden layers, preventing the attack from fully utilizing the attack budget. Conversely, small  $\beta$  can result in an excessively large distance between the perturbed representation and the original representation, making it difficult to reconstruct the perturbed representation within a given attack budget. When changing the hidden layer dimension  $h$  of the surrogate model, AHSG’s performance shows considerable fluctuation. Particularly, when the hidden layer dimension is small, the attack effectiveness decreases significantly. Because the hidden layers with a small dimension can not adequately capture the information of each node (including both primary and secondary semantics) for AHSG to utilize. However, it is worth noting that an attack graph generated using

a surrogate model with a large hidden layer dimension can still be effective when applied to a target model with a small hidden layer dimension.

### References

Bian, T.; Xiao, X.; Xu, T.; Zhao, P.; Huang, W.; Rong, Y.; and Huang, J. 2020. Rumor detection on social media with bi-directional graph convolutional networks. In *Proceedings of the AAAI conference on artificial intelligence*, volume 34, 549–556.

Chen, Y.; Yang, H.; Zhang, Y.; Ma, K.; Liu, T.; Han, B.; and Cheng, J. 2022. Understanding and Improving Graph Injection Attack by Promoting Unnoticeability. In *International Conference on Learning Representations*.

Dai, H.; Li, C.; Coley, C.; Dai, B.; and Song, L. 2019. Retrosynthesis prediction with conditional graph logic network. *Advances in Neural Information Processing Systems*, 32.

Dai, H.; Li, H.; Tian, T.; Huang, X.; Wang, L.; Zhu, J.; and Song, L. 2018. Adversarial attack on graph structured data. In *International conference on machine learning*, 1115–1124. PMLR.

Entezari, N.; Al-Sayouri, S. A.; Darvishzadeh, A.; and Papalexakis, E. E. 2020. All you need is low (rank) defending against adversarial attacks on graphs. In *Proceedings of the 13th international conference on web search and data mining*, 169–177.

Errica, F.; Podda, M.; Bacciu, D.; and Micheli, A. 2022. A Fair Comparison of Graph Neural Networks for Graph Classification. arXiv:1912.09893.

Fang, J.; Wen, H.; Wu, J.; Xuan, Q.; Zheng, Z.; and Chi, K. T. 2024. Gani: Global attacks on graph neural networks via imperceptible node injections. *IEEE Transactions on Computational Social Systems*.

Gao, J.; Gao, J.; Ying, X.; Lu, M.; and Wang, J. 2021. Higher-order interaction goes neural: A substructure assembling graph attention network for graph classification. *IEEE Transactions on Knowledge and Data Engineering*, 35(2): 1594–1608.

Gilmer, J.; Schoenholz, S. S.; Riley, P. F.; Vinyals, O.; and Dahl, G. E. 2017. Neural message passing for quantum chemistry. In *International conference on machine learning*, 1263–1272. PMLR.

Gosch, L.; Sturm, D.; Geisler, S.; and Günnemann, S. 2023. Revisiting Robustness in Graph Machine Learning. In *The Eleventh International Conference on Learning Representations (ICLR)*.

Hamilton, W.; Ying, Z.; and Leskovec, J. 2017. Inductive representation learning on large graphs. *Advances in neural information processing systems*, 30.

Jin, M.; Zheng, Y.; Li, Y.-F.; Gong, C.; Zhou, C.; and Pan, S. 2021a. Multi-Scale Contrastive Siamese Networks for Self-Supervised Graph Representation Learning. arXiv:2105.05682.

Jin, W.; Derr, T.; Wang, Y.; Ma, Y.; Liu, Z.; and Tang, J. 2021b. Node similarity preserving graph convolutional networks. In *Proceedings of the 14th ACM international conference on web search and data mining*, 148–156.



- Jin, W.; Ma, Y.; Liu, X.; Tang, X.; Wang, S.; and Tang, J. 2020. Graph structure learning for robust graph neural networks. In *Proceedings of the 26th ACM SIGKDD international conference on knowledge discovery & data mining*, 66–74.
- Kipf, T. N.; and Welling, M. 2017. Semi-Supervised Classification with Graph Convolutional Networks. arXiv:1609.02907.
- Liu, Z.; Luo, Y.; Wu, L.; Liu, Z.; and Li, S. Z. 2022. Towards Reasonable Budget Allocation in Untargeted Graph Structure Attacks via Gradient Debias. In *Advances in Neural Information Processing Systems*.
- Ma, C.; Ma, L.; Zhang, Y.; Sun, J.; Liu, X.; and Coates, M. 2020. Memory augmented graph neural networks for sequential recommendation. In *Proceedings of the AAAI conference on artificial intelligence*, volume 34, 5045–5052.
- Shen, Y.; Zhang, J.; Song, S.; and Letaief, K. B. 2022. Graph neural networks for wireless communications: From theory to practice. *IEEE Transactions on Wireless Communications*, 22(5): 3554–3569.
- Veličković, P.; Cucurull, G.; Casanova, A.; Romero, A.; Liò, P.; and Bengio, Y. 2018. Graph Attention Networks. arXiv:1710.10903.
- Wang, J.; Lukaszewicz, T.; Hu, X.; Cai, J.; and Xu, Z. 2021. Rsg: A simple but effective module for learning imbalanced datasets. In *Proceedings of the IEEE/CVF conference on computer vision and pattern recognition*, 3784–3793.
- Waniek, M.; Michalak, T. P.; Wooldridge, M. J.; and Rahwan, T. 2018. Hiding individuals and communities in a social network. *Nature Human Behaviour*, 2(2): 139–147.
- Wu, H.; Wang, C.; Tyshetskiy, Y.; Docherty, A.; Lu, K.; and Zhu, L. 2019. Adversarial Examples on Graph Data: Deep Insights into Attack and Defense. arXiv:1903.01610.
- Wu, M.; Pan, S.; and Zhu, X. 2021. Openwgl: open-world graph learning for unseen class node classification. *Knowledge and Information Systems*, 63(9): 2405–2430.
- Xiong, B.; Zhu, S.; Potyka, N.; Pan, S.; Zhou, C.; and Staab, S. 2022. Pseudo-Riemannian Graph Convolutional Networks. arXiv:2106.03134.
- Xu, K.; Chen, H.; Liu, S.; Chen, P.-Y.; Weng, T.-W.; Hong, M.; and Lin, X. 2019. Topology Attack and Defense for Graph Neural Networks: An Optimization Perspective. arXiv:1906.04214.
- Zhang, H.; Yuan, X.; Zhou, C.; and Pan, S. 2022. Projective ranking-based gnn evasion attacks. *IEEE Transactions on Knowledge and Data Engineering*, 35(8): 8402–8416.
- Zhou, W.; Liu, Y.; Zhao, L.; Xu, S.; and Wang, C. 2023. Pedestrian crossing intention prediction from surveillance videos for over-the-horizon safety warning. *IEEE Transactions on Intelligent Transportation Systems*.
- Zhu, D.; Zhang, Z.; Cui, P.; and Zhu, W. 2019. Robust graph convolutional networks against adversarial attacks. In *Proceedings of the 25th ACM SIGKDD international conference on knowledge discovery & data mining*, 1399–1407.
- Zügner, D.; Akbarnejad, A.; and Günnemann, S. 2018. Adversarial attacks on neural networks for graph data. In *Proceedings of the 24th ACM SIGKDD international conference on knowledge discovery & data mining*, 2847–2856.
- Zügner, D.; and Günnemann, S. 2019. Adversarial Attacks on Graph Neural Networks via Meta Learning. In *International Conference on Learning Representations (ICLR)*.